

Randomized Benchmarking under Different Gatesets

Kristine Boone,^{1,2} Arnaud Carignan-Dugas,^{1,2} Joel J. Wallman,^{1,2} and Joseph Emerson^{1,2,3}

¹*Institute for Quantum Computing and the Department of Applied Mathematics,
University of Waterloo, Waterloo, Ontario N2L 3G1, Canada*

²*Quantum Benchmark Inc., 51 Breithaupt, Kitchener, Ontario, Canada N2H5G5*

³*Canadian Institute for Advanced Research, Toronto, Ontario M5G 1Z8, Canada*

We provide a comprehensive analysis of the differences between two important standards for randomized benchmarking (RB): the Clifford-group RB protocol proposed originally in Emerson et al (2005) and Dankert et al (2006), and a variant of that RB protocol proposed later by the NIST group in Knill et al, PRA (2008). While these two protocols are frequently conflated or presumed equivalent, we prove that they produce distinct exponential fidelity decays leading to differences of up to a factor of 3 in the estimated error rates under experimentally realistic conditions. These differences arise because the NIST RB protocol does not satisfy the unitary two-design condition for the twirl in the Clifford-group protocol and thus the decay rate depends on non-invariant features of the error model. Our analysis provides an important first step towards developing definitive standards for benchmarking quantum gates and a more rigorous theoretical underpinning for the NIST protocol and other RB protocols lacking a group-structure. We conclude by discussing the potential impact of these differences for estimating fault-tolerant overheads.

I. INTRODUCTION

Clifford-group randomized benchmarking (RB) [1, 2] has become the *de facto* standard tool for assessing and optimizing the quantum control required for quantum computing systems by estimating error rates associated with sets of elementary gates operations. It has been known for some time that this protocol leads to an invariant exponential decay [1–3] because it is equivalent to a sequence of twirls [3] with unitary-two designs [2]. More recently, the robustness of the Clifford-group RB protocol has been supported by a rigorous theoretical framework, including proofs that an exponential fidelity decay will be observed under very broad experimental conditions, including essentially arbitrary state preparation and measurement errors [4, 5] and gate-dependent errors [6], as well as proofs that the observed error rate relates directly to a well-defined notion of gate-fidelity [6–8], which fully overcome recent concerns about relating measured RB error rates to a meaningful concept of gate-fidelity under gate-dependent errors [7].

While a wide-variety of group-based generalizations of RB have been proposed in recent years, *e.g.* [6, 9–13], in this Letter we focus on clarifying the physical relevance of a standing conflation in the literature between the now standard Clifford-group RB protocol proposed in [1, 2] and an alternate version of RB proposed later by NIST [14]. As described below, these are distinct protocols that measure distinct properties of the error model and thus can produce different error rate estimates under the same, realistic experimental conditions. Moreover, because the NIST protocol does not admit a closed-group or unitary two-design structure, the rigorous theoretical framework justifying Clifford-group RB does not trivially extend to support the physical interpretation and robustness of NIST RB.

In this Letter we identify the operationally-relevant differences between the Clifford-group RB protocol and the

NIST version of RB which clarifies how they can lead to very different error rate estimates given the same error model (as defined in terms of the elementary control pulses). We then provide the first rigorous proof that the NIST RB protocol does indeed produce an exponential decay under gate-independent error models. This is an important step toward developing a theoretical justification for the NIST protocol and other RB protocols that do not admit a group-structure in the case of gate-dependent errors and the ultimate goal of a theoretical framework within which error reconstruction under RB protocols with different gate sets can be extracted in a unified and consistent manner. Our analysis is thus also essential for comparing cross-platform benchmarking methods and standards for quantum computing. As a second contribution, we numerically explore the size and scope of the quantitative differences in estimated error rates that arise under each of the protocols for a variety of physically relevant error models and pulse-decompositions, and observe that experimentally estimated error rates can differ by as much as a factor of 3 in typical cases. We conclude by discussing how these differences are relevant for detecting gate-dependent errors, and estimating fault-tolerant overheads under quantum error correction.

II. BACKGROUND AND MOTIVATION

The original proposal for randomized benchmarking from Emerson *et al.* [1] considered implementing long sequences of quantum gates drawn *uniformly* at random from the group $SU(d)$ for any quantum systems with Hilbert space dimension d . That work proved that the measured fidelity would follow an exponential decay with a decay rate that is fixed uniquely by the error model, that is, the measured decay rate would not depend on the choice of initial state or the specific random quantum gate sequences.

Protocol 1: Standard Clifford-group RB, as described in [1, 2].

1. Sample a set of m gates G_i picked independently and uniformly at random from the Clifford group \mathbf{C} defined in eq. (5);
2. Determine the recovery gate G_{m+1} (see text below);
3. Prepare a state $\rho \approx |0\rangle\langle 0|$;
4. Perform the sampled gates from step 1, followed by the recovery gate G_{m+1} determined in step 2:
 $\tilde{G}_{m+1:1} = \tilde{G}_{m+1} \circ \dots \circ \tilde{G}_1$;
5. Measure a POVM $\{Q, \mathbb{I} - Q\}$, where the first observable is $Q \approx G_{m+1:1}(|0\rangle\langle 0|)$, and respective outcome labels are {"recovery", "non-recovery"};
6. Repeat steps 3–5 a number of times to estimate the probability of observing the "recovery" event $\Pr(\text{"recovery"} | \{G_i\}, m) = \text{Tr } Q \tilde{G}_{m+1:1}(\rho)$;
7. Repeat steps 1–6 for s different sets of m randomly sampled gates $\{G_i\}$;
8. Repeat steps for 1–7 for different values of m of random gates.
9. Fit the estimated recovery probabilities to the decay model

$$A_{\mathbf{C}} p_{\mathbf{C}}^m + B_{\mathbf{C}} ; \quad (1)$$

10. Estimate the Clifford gate-set infidelity through

$$r_{\mathbf{C}} = (1 - p_{\mathbf{C}})/2 . \quad (2)$$

This protocol suffered from two limitations: the random gates were drawn from a continuous set, which is impractical even for $d = 2$, and the protocol would not be efficient for large systems because a typical random element of $\text{SU}(d)$ requires exponentially long gate sequences under increasing numbers of qubits. Additionally, in that limit the inversion gate may not be computed efficiently.

However, practical and efficient solutions to both of these problems were proposed in Dankert *et al.* [2] in 2006, which proved and observed that drawing gates uniformly at random from the Clifford group would lead to the same exponential decay rate as computed in the protocol proposed earlier in Emerson *et al.* [1], which follows from the unitary 2-design property of the Clifford group. This connection is made more explicit through the observation that a random sequence of gates drawn from any group is equivalent to an independent sequence of twirls under that group, as shown explicitly in [3] and had been conjectured earlier in [1].

Protocol 2: NIST RB, as described in [14].

1. Sample a set of m gates G_i picked independently and uniformly at random from the NIST gate-set \mathbf{N} defined in eq. (8);
- 2–8. Idem as in protocol 1.
9. Fit the estimated recovery probabilities to the decay model

$$A_{\mathbf{N}} p_{\mathbf{N}}^m + B_{\mathbf{N}} . \quad (3)$$

10. Estimate the NIST gate-set infidelity through

$$r_{\mathbf{N}} = (1 - p_{\mathbf{N}})/2 . \quad (4)$$

Collectively these papers define what is now known as Clifford-group RB, an efficient and practical method for assessing error rates for quantum processors on arbitrarily large numbers of qubits, summarized here as Protocol 1. This Clifford-group RB protocol has become a *de facto* standard for benchmarking and optimizing gate performance and has been implemented by a large number of groups across various hardware platforms to characterize single- and multi-qubit gate operations, see, *e.g.*, Refs [15–21].

The theoretical underpinnings of the standard protocol were clarified and further developed by Magesan *et al.* [4, 5], which showed that the exponential decay rate was robust to state preparation and measurement errors (SPAM), and by Wallman [6] and Dugas *et al.* [8], which showed that the exponential decay rate was meaningfully related to a gate-fidelity in spite of the gauge freedom highlighted by Proctor *et al.* [7] that occurs in the usual definition of the average gate-fidelity. Additionally, the work of Wallman [6] established that the RB error rate is robust to very large variations in the error model over the gate set (known as gate-dependent error models) and thus established that RB can also be an effective tool for diagnosing non-Markovian errors. This follows from the fact that only non-Markovian errors (including what are sometimes called time-dependent Markovian errors) can produce a statistically significant deviation from an exponential decay under a Clifford-group RB experiment.

A different version of the 2005 Emerson *et al.* [1] protocol was proposed by Knill *et al.* [14] in 2008 and implemented in the NIST ion trap. This proposal involved the same kind of motion reversal experiment proposed in Emerson *et al.* [1] but selects a random sequences of gates drawn from a *non-uniform* sampling of the single-qubit Cliffords, defined as "Pauli-randomized $\pi/2$ gates". The precise recipe for this protocol is summarized as Protocol 2. The NIST version of the randomized benchmarking protocol continues to be implemented mainly in ion traps [22, 23]. We note that in contrast to the earlier Clifford-group RB protocol which is defined for single- and multi-qubit gate operations, the NIST version of RB

is defined only for single-qubit gate operations. In this Letter, we prove that the measured fidelity under the NIST protocol will follow an exponential decay, which has never been established for this protocol, and relate the decay rate to the intrinsic properties of the error model, demonstrating how it differs from the properties measured by Clifford-group RB. This analysis also provides first step towards developing a self-consistent theoretical framework for interpreting and relating the results of the large and growing family of RB-style protocols, which all share the structure of applying random sequences of gates and differ mainly through the choice of which random gate-sets [5, 6, 9–13, 20, 24–29].

Finally, an additional motivation for the present work comes from the recent conceptual development [30] establishing how accurately RB error estimation methods can inform the design and ‘in vivo’ performance of large-scale quantum computations. This development overcomes a standing criticism of RB protocols that the very nature of a randomization protocol limits these protocols to detect only the stochastic component of coherent errors - and hence that RB-type protocols are not able to capture the full impact of these errors. Coherent errors are those that typically arise from imperfect quantum control due to residual mis-calibrations¹ and pose a major challenge for reliable quantum computation. However, this perceived limitation has become a strength of RB protocols thanks to the concept of randomized compiling [30]. Randomized compiling is an important generalization and improvement to the concept of Pauli-Frame Randomization (PFR) proposed earlier in [31] that does not require any overhead for the randomization and works for universal gate sets². When implementing a quantum algorithm via randomized compiling, the only performance limiting component of a coherent error is precisely the stochastic component that is detected via RB protocols. In summary, a precise and accurate understanding of RB error estimates is highly relevant because RB detects precisely the component of the error that determines the ‘in vivo’ performance of the gate operations within a large-scale circuit performed via randomized compiling.

III. RESULTS

A. Standard RB vs NIST RB

The standard RB protocol (SRB) [1, 2] is summarized in protocol 1. The recovery operations mentioned in step

2 is usually an inversion gate, where $G_{m+1} = G_{m:1}^{-1}$, in which case the recovery observable simply corresponds to the initial state: $Q \approx |0\rangle\langle 0|$. However, performing the inverse only up to a random bit flip (i.e $G_{m+1} = X_\pi^b G_{m:1}^{-1}$) leads to a simpler decay model with less free parameters because then $B = 1/2$. Of course in this case one has to keep track of the bit flip, that is $Q \approx X_\pi^b(|0\rangle\langle 0|)$. Such a randomized recovery operation was proposed originally in [14].

SRB is typically implemented using the Clifford group \mathbf{C} as a randomizing gate-set, as specified in the first step of protocol 1, but the derivation of the decay model shown in eq. (1) holds for any unitary 2-design [2]. The Clifford group is defined as follows. First consider the pulses along any Cartesian axis system

$$X_\theta := e^{-i\theta/2} \sigma_x, \quad Y_\theta := e^{-i\theta/2} \sigma_y, \quad Z_\theta := e^{-i\theta/2} \sigma_z,$$

where σ_i denote the unitary Pauli matrices. The Pauli group \mathbf{P} is defined in terms of the identity operation and 3 elementary π pulses: $\mathbf{P} := \{\mathbb{I}, X_\pi, Y_\pi, Z_\pi\}$. The Clifford group \mathbf{C} is defined as the normalizer of the Pauli group and can be obtained from the Pauli group composed with the coset $\mathbf{S} := \{\mathbb{I}, X_{\pi/2}, Y_{\pi/2}, Z_{\pi/2}, Z_{\pi/2}X_{\pi/2}, X_{-\pi/2}Z_{-\pi/2}\}$:

$$\mathbf{C} := \mathbf{S} \cdot \mathbf{P} = \{S \circ P \mid S \in \mathbf{S}, P \in \mathbf{P}\}. \quad (5)$$

Some other experimental groups performed RB using alternate 2-design gate-sets in step 1 of protocol 1[18]. Amongst the set of possible unitary 2-designs, it is worth mentioning those following subsets of \mathbf{C} . Consider the cyclic group $\mathbf{T} := \{\mathbb{I}, Z_{\pi/2}X_{\pi/2}, X_{-\pi/2}Z_{-\pi/2}\}$, then the following sets both form 2-designs of order 12:

$$\mathbf{C}_{12} := \mathbf{T} \cdot \mathbf{P} = \{T \circ P \mid T \in \mathbf{T}, P \in \mathbf{P}\}, \quad (6)$$

$$\sqrt{2}\mathbf{C}_{12} := Z_{\pi/2} \cdot \mathbf{C}_{12} = \{Z_{\pi/2} \circ C \mid C \in \mathbf{C}_{12}\}, \quad (7)$$

with $\mathbf{C}_{12} \cup \sqrt{2}\mathbf{C}_{12} = \mathbf{C}$. Obviously, the decay parameters as well as the infidelity depend on the randomizing gate-set (hence the indices). The validity of the decay model and the connection between the decay parameter and the gate-set infidelity have been demonstrated in the case of gate-independent Markovian noise scenarios in [1]. The proofs of eq. (1) and eq. (2) have been generalized to encompass gate-dependent noise scenarios in [6, 32] and [8] respectively³. Although the proof techniques can get mathematically heavy, their essence remains simple: the algebraic richness of 2-designs prevents errors to accumulate in an unpredictable way as the circuit grows in length. As we show with more care in the next section, the random sampling over the gate-set tailors the effective errors at each cycle in a depolarizing channel

¹ Note that cross-talk is a non-trivial coherent error that results from control errors affecting distant qubits.

² In particular, relative to PFR, randomized compiling (i) does not add additional overhead to each clock cycle, which it achieves by ‘compiling in’ the randomizing gates, (ii) works for universal gate sets, and (iii) rigorously characterizes how close the effective error model is to a purely stochastic error model under errors gate-dependent errors

³ In gate-dependent noise scenarios, the connection between the RB decay parameter and the gate-set infidelity remains a (strongly supported) conjecture for $d > 2$.

for which the evolution is parameterized by a single real number p . The errors are stripped out of all their properties except one, which turns out to be in one-to-one correspondence with their average infidelity. By modifying the sampled circuits lengths, we can estimate the parameter p and retrieve the infidelity.

While unitary 2-designs are provably effective randomizing gate-sets, leading to the model portrayed in eq. (1), some algebraically weaker gate-sets have indicated a similar exponential decaying behaviour.

The gate-set \mathbf{N} used in NIST RB [14] is a composition of a set $\mathbf{Q} := \{X_{\pm\pi/2}, Y_{\pm\pi/2}\}$, consisting of $\pi/2$ pulses in the xy-plane, with the Pauli operators:

$$\mathbf{N} := \mathbf{Q} \cdot \mathbf{P} = \{Q \circ P \mid Q \in \mathbf{Q}, P \in \mathbf{P}\}. \quad (8)$$

\mathbf{N} has order 8, and although it contains all its inverse elements (that is $\forall N \in \mathbf{N}, \exists M \in \mathbf{N} \text{ s.t. } M \cdot N = \mathbb{I}$), it is not closed under multiplication. It does not form a group, nor a 2-design; however, the closure $\langle \mathbf{N} \rangle$ forms the Clifford group \mathbf{C} .

RB sequences can be seen as Markov chains [33], where the elements of the chain are the aggregate circuits, that is $C_1 = G_1$, $C_2 = G_2 G_1$, $C_m = G_{m:1}$. Indeed, the probability distribution on circuits $C_m = G_{m:1}$ simply depends on the circuit C_{m-1} and on the probability distribution of the random gate applied at step m . In standard RB, C_i is always uniformly distributed over the Clifford group. In NIST RB, C_{2n} (or C_{2n+1}) converges to a uniform distribution over \mathbf{C}_{12} (or $\sqrt{\mathbf{Z}}\mathbf{C}_{12}$), as shown in fig. 1.

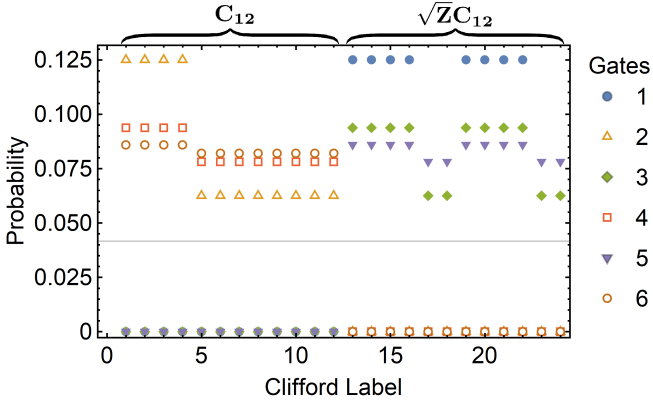


FIG. 1. Probability distribution over the Clifford gates \mathbf{C} (labelled as in [18]) after m gates (i.e clock cycles) of NIST RB drawn uniformly at random from $\mathbf{N} \subset \mathbf{C}$. This leads to a *non-uniform* sampling over the Cliffords that varies as m increases. Asymptotically, for a sequence of even (or odd) length, the probability distribution tends toward a uniform distribution over \mathbf{C}_{12} (or $\sqrt{\mathbf{Z}}\mathbf{C}_{12}$). The grey line indicates an equal probability over the full 24 Clifford group \mathbf{C} .

While this approach to RB has been useful for estimating error rates [14, 22, 23], in the absence of a unitary 2-design structure, it is not clear how to relate the measured probabilities from protocol 2 to the usual decay predicted under SRB, or to any infidelity for that matter. In this paper we provide a concrete analysis of the

outcome of protocol 2, which yields a justification and interpretation for the decay model eqs. (3) and (4).

It is important to emphasize that NIST RB now falls into a family of RB protocols defined as “direct RB” [27]. The analysis below gives a concrete instance of direct RB that both justifies and interprets past experiments and gives an insightful example of the main idea behind direct RB.

B. Theoretical Analysis of NIST RB

The goal of this section is to provide the key insight behind the mechanics of NIST RB. To lighten up the mathematical machinery, we assume a gate-independent error model⁴, where the noisy gates are followed by an error Λ :

$$\tilde{G} = \Lambda G. \quad (9)$$

In such model, the gate-set infidelities $r_{\mathbf{C}}$ and $r_{\mathbf{N}}$ are *de facto* equal to the infidelity of the error $r(\Lambda, \mathbb{I})$. We proceed in showing that $r(\Lambda, \mathbb{I})$ can be estimated by both protocols 1 and 2.

The recovery probabilities look like

$$\text{Tr } Q \Lambda \underbrace{X_{\pi}^b G_{m:1}^{-1}}_{G_{m+1}} \Lambda G_m \cdots \Lambda G_2 \Lambda G_1(\rho). \quad (10)$$

Shoving the last error Λ as well as the random bit flip X_{π}^b in the measurement procedure (that is, $Q \rightarrow X_{\pi}^b \Lambda^{\dagger}(Q)$), leaves us with the random sequence which is at the heart of both NIST RB and SRB protocols:

$$S(\{G_i\}) = G_{m:1}^{-1} \Lambda G_m \cdots \Lambda G_2 \Lambda G_1. \quad (11)$$

In SRB, the next step in the analysis consists in redefining the gates as $G_i = G'_i G'_{i-1}^{-1}$ (with $G_1 = G'_1$), where both G_i and G'_i are picked uniformly at random from the randomizing set. Such a relabeling is possible because the randomizing gate-set is usually a group. Averaging over all sequences yields

$$\begin{aligned} \mathbb{E}_{\{G_i\}} S(\{G_i\}) &= \mathbb{E}_{\{G'_i\}} G_{m:1}^{-1} \Lambda G'_m \cdots G'_2^{-1} \Lambda G'_2 G'_1^{-1} \Lambda G'_1 \\ &= (\Lambda^{\mathbf{C}})^m, \end{aligned} \quad (12)$$

where

$$\Lambda^{\mathbf{C}} := \frac{1}{|\mathbf{C}|} \sum_{G \in \mathbf{C}} G^{-1} \Lambda G \quad (13)$$

is referred to as the twirl of the error Λ over the gate-set \mathbf{C} . If \mathbf{C} is a 2-design, then the twirled channel $\Lambda^{\mathbf{C}}$

⁴ The formal analysis of direct RB under more general gate-dependent noise scenarios will be considered in subsequent work. However, in appendix A we elucidate the broad reasoning required for a gate-dependent analysis.

is reduced to a depolarizing channel. To mathematically concretize the description of a channel Λ , we resort to the 4×4 Pauli-Liouville representation, which is defined as

$$\Lambda_{ij} := \frac{1}{2} \text{Tr } B_j^\dagger \Lambda(B_i) \quad (14)$$

where $B_1 = \mathbb{I}$, $B_2 = \hat{\sigma}_x$, $B_3 = \hat{\sigma}_y$, $B_4 = \hat{\sigma}_z$. In such representation, the depolarizing channel $\Lambda^{\mathbf{C}}$ is expressed as a diagonal matrix $\text{diag}(1, p_{\mathbf{C}}, p_{\mathbf{C}}, p_{\mathbf{C}})$, where $p_{\mathbf{C}}$ is a real number close to 1:

$$p_{\mathbf{C}} = \frac{\Lambda_{22} + \Lambda_{33} + \Lambda_{44}}{3}. \quad (15)$$

The averaged core sequence hence evolves as

$$\mathbb{E}_{\{G_i\}} S(\{G_i\}) = (\Lambda^{\mathbf{C}})^m = \text{diag}(1, p_{\mathbf{C}}^m, p_{\mathbf{C}}^m, p_{\mathbf{C}}^m). \quad (16)$$

Deriving eq. (1) is then simply a matter of incorporating SPAM procedures in the evaluation of the recovery probabilities. Straightforward algebra links the infidelity of Λ with its diagonal Liouville matrix elements through

$$r(\Lambda, \mathbb{I}) = \frac{1}{2} - \frac{\Lambda_{22} + \Lambda_{33} + \Lambda_{44}}{6}. \quad (17)$$

The relation between the decay constant $p_{\mathbf{C}}$ and the gate-set infidelity $r_{\mathbf{C}} = r(\Lambda, \mathbb{I})$ results from combining eq. (15) and eq. (17).

The relabeling trick resulting in a m -composite depolarizing channel is not possible in NIST RB: \mathbf{N} is neither a group nor a 2-design. However, although \mathbf{N} has a weaker algebraic structure, it is not completely devoid of interesting properties. Indeed, every element of \mathbf{N} can be written as $P_{\text{left}} \cdot Q \cdot P_{\text{right}}$, where $P_{\text{left}}, P_{\text{right}} \in \mathbf{P}$ and $Q \in \mathbf{Q}$. Using this, we can relabel every gate G_i as

$$G_1 = P_1 Q_1, \quad (18a)$$

$$G_i = P_i Q_i P_{i-1}^{-1} \quad (i = 2, \dots, m), \quad (18b)$$

$$G_{m+1}^{-1} = Q_{m+1}^{-1} P_m^{-1} \quad (18c)$$

where P_i is chosen UAR from the Pauli group \mathbf{P} , and Q_i are chosen UAR from \mathbf{Q} . Using such a manipulation and randomizing over the Paulis transform the core sequence into

$$\mathbb{E}_{\{P_i\}} S(\{G_i\}) = Q_{m+1}^{-1} \Lambda^{\mathbf{P}} Q_m \cdots \Lambda^{\mathbf{P}} Q_2 \Lambda^{\mathbf{P}} Q_1, \quad (19)$$

where $\Lambda^{\mathbf{P}}$ is the error channel twirled over the Pauli group. In the Pauli-Liouville picture, the Pauli group has 4 inequivalent irreps; the twirled channel is diagonal:

$$\Lambda^{\mathbf{P}} = \text{diag}(1, x, y, z), \quad (20)$$

where $x = \Lambda_{22}$, $y = \Lambda_{33}$, $z = \Lambda_{44}$. The relabeling method still can't be used with the Q_i 's, but the simplification of the noise channel Λ through the Pauli twirl unveils a recursive approach. Consider the $m = 1$ case:

$$\mathbb{E}_{\{G_1\}} S(\{G_1\}) = \mathbb{E}_{\{Q_1\}} Q_1^{-1} \Lambda^{\mathbf{P}} Q_1 = \Lambda^{\mathbf{N}}, \quad (21)$$

where the twirl over the NIST gate-set results in

$$\Lambda^{\mathbf{N}} = \text{diag}\left(1, \frac{x+z}{2}, \frac{y+z}{2}, \frac{x+y}{2}\right). \quad (22)$$

The $m = 2$ case suggests a recursion relation:

$$\mathbb{E}_{\{G_i\}} S(\{G_i\}) = (\Lambda^{\mathbf{N}} \Lambda^{\mathbf{P}})^{\mathbf{N}}, \quad (23a)$$

$$(\Lambda^{\mathbf{N}} \Lambda^{\mathbf{P}})^{\mathbf{N}} = \text{diag}(1, x_2, y_2, z_2), \quad (23b)$$

where

$$x_2 = \frac{x \frac{(x+z)}{2} + z \frac{(x+y)}{2}}{2}, \quad (24a)$$

$$y_2 = \frac{y \frac{(y+z)}{2} + z \frac{(x+y)}{2}}{2}, \quad (24b)$$

$$z_2 = \frac{x \frac{(x+z)}{2} + y \frac{(y+z)}{2}}{2}. \quad (24c)$$

Indeed, the general case can be expressed as

$$\mathbb{E}_{\{G_i\}} S(\{G_i\}) = \left(\left((\Lambda^{\mathbf{N}} \Lambda^{\mathbf{P}})^{\mathbf{N}} \Lambda^{\mathbf{P}} \right)^{\mathbf{N}} \Lambda^{\mathbf{P}} \cdots \right)^{\mathbf{N}}, \quad (25a)$$

$$\left(\left((\Lambda^{\mathbf{N}} \Lambda^{\mathbf{P}})^{\mathbf{N}} \Lambda^{\mathbf{P}} \right)^{\mathbf{N}} \Lambda^{\mathbf{P}} \cdots \right)^{\mathbf{N}} = \text{diag}(1, x_m, y_m, z_m), \quad (25b)$$

where the recursion relation can be stated as

$$x_m = \frac{x \cdot x_{m-1} + z \cdot z_{m-1}}{2}, \quad (26a)$$

$$y_m = \frac{y \cdot y_{m-1} + z \cdot z_{m-1}}{2}, \quad (26b)$$

$$z_m = \frac{x \cdot x_{m-1} + y \cdot y_{m-1}}{2}. \quad (26c)$$

Using basic linear algebra, this system of recursive equations can be expressed as

$$\begin{bmatrix} x_m \\ y_m \\ z_m \end{bmatrix} = M \begin{bmatrix} x_{m-1} \\ y_{m-1} \\ z_{m-1} \end{bmatrix} = M^m \begin{bmatrix} 1 \\ 1 \\ 1 \end{bmatrix}, \quad (27)$$

where

$$M = \frac{1}{2} \begin{bmatrix} x & 0 & z \\ 0 & y & z \\ x & y & 0 \end{bmatrix}. \quad (28)$$

x, y and z differ from 1 by at most order $r(\Lambda, \mathbb{I})$. Hence, up to the second order in the infidelity, M has the following spectrum:

$$\lambda_1 \approx \frac{x+y+z}{3} = p_{\mathbf{C}}, \quad (29a)$$

$$\lambda_2 \approx \frac{x+y}{4}, \quad (29b)$$

$$\lambda_3 \approx -\frac{x+y+4z}{12}. \quad (29c)$$

Since $\lambda_1 \approx 1$, $\lambda_2 \approx 1/2$ and $\lambda_3 \approx -1/2$, M^m converges very quickly to a rank-1 operator as m increases. This means that for m large enough so that $1/2^m$ becomes negligible, x_m, y_m, z_m are proportional to λ_1^m :

$$\mathbb{E}_{\{G_i\}} S(\{G_i\}) \approx \text{diag}(1, c_1 \lambda_1^m, c_2 \lambda_1^m, c_3 \lambda_1^m), \quad (30)$$

where c_i are proportionality constants. Equation (3) is obtained by incorporating the SPAM procedures in evaluating the recovery probabilities, and by relabeling λ_1 as $p_{\mathbf{N}}$. Finally, the relation between the decay $p_{\mathbf{N}}$ and the gate-set infidelity $r_{\mathbf{N}} = r(\Lambda, \mathbb{I})$ is retrieved via eq. (29a):

$$r_{\mathbf{N}} = (1 - p_{\mathbf{N}})/2 + O(r_{\mathbf{N}}^2), \quad (31)$$

which essentially states that the NIST RB decay parameter $p_{\mathbf{N}}$ provides a very good estimates of the gate-set infidelity $r_{\mathbf{N}}$ through eq. (4).

With this analysis behind us, let's compare the internal mechanics of protocols 1 and 2. First of all, both protocols make use of randomizing gate-sets, \mathbf{C} and \mathbf{N} respectively. In both cases, the randomization tailors the error dynamics such that the average core sequence $\mathbb{E}_{\{G_i\}} S(\{G_i\})$ evolves with respect to a single decay parameter, as show in eqs. (16) and (30). An interesting difference here is that the Clifford randomization simplifies the error into a 1-parameter depolarizing channel at each time step, while the NIST randomization doesn't, as shown in eq. (22). In the latter case, certain error components remain "imperfectly shuffled" after a few random gates, leaving space for a multi-parameterized noise evolution portrayed by eqs. (27) and (28). However, as the random sequence gets longer, the evolution quickly converges to a 1-parameter decay. The fact that this decay relates to the infidelity shouldn't be surprising, since $\text{diag}(0, 1, 1, 1)$ is a channel component that commutes with every unitary (so is "immuned" to twirling). Given an error Λ , its corresponding coefficient is $(\Lambda_{22} + \Lambda_{33} + \Lambda_{44})/3$, which is in one-to-one correspondence with the infidelity $r(\Lambda, \mathbb{I})$ via eq. (17).

C. Measured Error Rates under NIST RB vs SRB

In the previous section, we showed that under the assumption of gate-independent errors, the gate-set infidelities $r_{\mathbf{C}}$ and $r_{\mathbf{N}}$ could be estimated via SRB and NIST RB respectively, and that these estimates did both coincide with $r(\Lambda, \mathbb{I})$. In reality, one might find through experiment that $r_{\mathbf{C}}$ and $r_{\mathbf{N}}$ differ quite substantially. This, of course, is explained by gate-dependent effects: certain gates have higher infidelities than others, and since $r_{\mathbf{C}}$ and $r_{\mathbf{N}}$ consist in the expected gate infidelity *over their respective gate-set* (see appendix A for further justifications), they will yield different values.

To demonstrate this, we numerically simulated both SRB and NIST RB experiments implemented in different fashions, using a plethora of primitive pulse sets (see table I) each undergoing various physically realistic gate-dependent noise scenarios. The respective infidelities $r_{\mathbf{C}}$

Index	Pulse Set	$n_{\mathbf{C}}$	$n_{\mathbf{N}}$
1	$\{\mathbb{I}, \tilde{X}_{+\pi/2}, \tilde{Y}_{+\pi/2}\}$	3.08333	4.0
2	$\{\tilde{X}_{\pm\pi/2}, \tilde{Y}_{\pm\pi/2}\}$	2.25	3.5
3	$\{\mathbb{I}, \tilde{X}_{\pm\pi/2}, \tilde{Y}_{\pm\pi/2}\}$	2.16667	3.0
4	$\{\tilde{X}_{\pi}, \tilde{Y}_{\pi}, \tilde{X}_{\pm\pi/2}, \tilde{Y}_{\pm\pi/2}\}$	1.91667	2.5
5	$\{\tilde{\mathbb{I}}, \tilde{Z}_{\pi}, \tilde{X}_{\pm\pi/2}, \tilde{Y}_{\pm\pi/2}\}$	1.91667	2.5
6	$\{\tilde{\mathbb{I}}, \tilde{X}_{\pi}, \tilde{Y}_{\pi}, \tilde{X}_{\pm\pi/2}, \tilde{Y}_{\pm\pi/2}\}$	1.875	2.25
7	$\{\tilde{\mathbb{I}}, \tilde{X}_{\pi}, \tilde{Y}_{\pi}, \tilde{Z}_{\pi}, \tilde{X}_{\pm\pi/2}, \tilde{Y}_{\pm\pi/2}\}$	1.8333	2.0
8	$\{\mathbb{I}, Z_{\pi}, \tilde{X}_{\pm\pi/2}, \tilde{Y}_{\pm\pi/2}\}$	1.66667	2.0
9	$\{\mathbb{I}, \tilde{X}_{\pi}, \tilde{Y}_{\pi}, Z_{\pi}, \tilde{X}_{\pm\pi/2}, \tilde{Y}_{\pm\pi/2}\}$	1.58333	1.5

TABLE I. Each of the 24 \mathbf{C} s and 8 \mathbf{N} s were constructed by a sequence of noisy ($\tilde{\mathbb{I}}, \tilde{X}_{\theta}, \tilde{Y}_{\theta}, \tilde{Z}_{\theta}$) and virtually (ideal) implemented ($\mathbb{I}, X_{\theta}, Y_{\theta}, Z_{\theta}$) pulses. Note that when implementing the π pulses, the direction of rotation (sign of π) is selected uniformly at random as described in [14]. $n_{\mathbf{C}}$ and $n_{\mathbf{N}}$ are the average number of noisy pulses per gate from \mathbf{C} and \mathbf{N} , and is used for calculating the scaled infidelity ($r_{\mathbf{C}}/n_{\mathbf{C}}$ and $r_{\mathbf{N}}/n_{\mathbf{N}}$).

and $r_{\mathbf{N}}$ are juxtaposed in fig. 2, and differ by up to a factor of ~ 3 . This might not strike as a major difference in a day and age where the infidelity is typically filtered through its order of magnitude. That being said, for both surface and concatenated quantum error correcting codes, the overhead becomes more sensitive to the error rate as it approaches the fault-tolerant threshold. Therefore, a factor of 3 could dramatically increase the overhead (by more than an order of magnitude) if the error rate is close to the threshold. In the extreme case, the factor of 3 could cause the error rate to surpass the threshold and fault tolerance would become impossible.

One might be tempted to reconcile those different infidelities by accounting for the number of primitive pulses that form each gate-set element. That is, if the Clifford gates $C \in \mathbf{C}$ necessitate the average application of $n_{\mathbf{C}} = 1.875$ pulses and that the NIST gates $N \in \mathbf{N}$ require an average of $n_{\mathbf{N}} = 2.25$ pulses, it might seem natural to scale the infidelities as $r_{\mathbf{C}}/n_{\mathbf{C}}$ and $r_{\mathbf{N}}/n_{\mathbf{N}}$.

This is a common misconception because scaling the infidelity is only meaningful if it grows linearly with the number of pulses, as is the case of purely stochastic error. For example, in gate-dependent dephasing scenarios, the scaled infidelities ($r_{\mathbf{C}}/n_{\mathbf{C}}$ and $r_{\mathbf{N}}/n_{\mathbf{N}}$) only differ by $O(r_{\mathbf{N}}^2)$ because the error is purely stochastic (incoherent) and pulse-independent (see fig. 3c).

Contrarily, it has been shown that under coherent error scenarios, the composite errors can vary [34], as they can positively and negatively interfere. Therefore, when the error is coherent, NIST RB and SRB obtain different scaled infidelities, despite the infidelity per pulse remain-

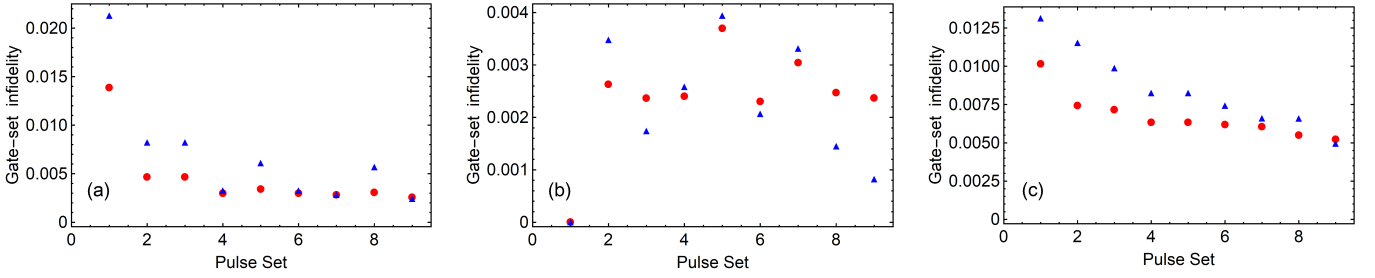


FIG. 2. (Color online) A comparison between the gate-set infidelities r_N (blue triangles) and r_C (red points) for pulse sets from table I with gate-dependent (a) coherent over-rotation error $\tilde{I} = \mathbb{I}$, $\tilde{X}_{\pm\theta} = X_{\pm(\theta+0.1)}$, $\tilde{Y}_{\pm\theta} = Y_{\pm(\theta+0.1)}$, $\tilde{Z}_{\pm\theta} = Z_{\pm(\theta+0.1)}$ (b) coherent Z-rotation error $\tilde{I} = Z_{0.1}$, $\tilde{X}_{\theta} = Z_{0.1}X_{\theta}$, $\tilde{Y}_{\theta} = Z_{0.1}Y_{\theta}$, $\tilde{Z}_{\theta} = Z_{\theta+0.1}$, and (c) incoherent dephasing error $\tilde{I} = D_{0.99}$, $\tilde{X}_{\theta} = D_{0.99}X_{\theta}$, $\tilde{Y}_{\theta} = D_{0.99}Y_{\theta}$, $\tilde{Z}_{\theta} = D_{0.99}Z_{\theta}$, where $D_{\alpha} = \text{diag}(1, \alpha, \alpha, 1)$. Under these error models and pulse sets, r_N and r_C differ by up to a factor of 3, which could significantly affect the expected overhead under quantum error correction.

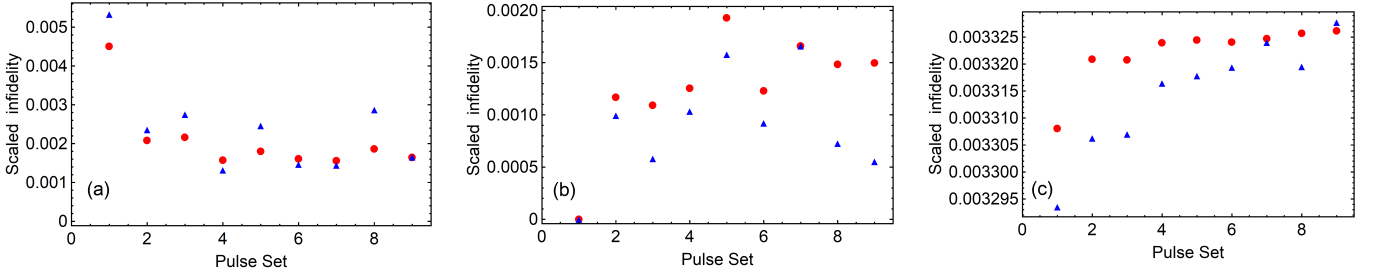


FIG. 3. (Color online) A comparison between the scaled infidelities r_N/n_N (blue triangles) and r_C/n_C (red points) using pulse sets from table I with gate-dependent (a) coherent over-rotation error $\tilde{I} = \mathbb{I}$, $\tilde{X}_{\pm\theta} = X_{\pm(\theta+0.1)}$, $\tilde{Y}_{\pm\theta} = Y_{\pm(\theta+0.1)}$, $\tilde{Z}_{\pm\theta} = Z_{\pm(\theta+0.1)}$ (b) coherent Z-rotation error $\tilde{I} = Z_{0.1}$, $\tilde{X}_{\theta} = Z_{0.1}X_{\theta}$, $\tilde{Y}_{\theta} = Z_{0.1}Y_{\theta}$, $\tilde{Z}_{\theta} = Z_{\theta+0.1}$, and (c) incoherent dephasing error $\tilde{I} = D_{0.99}$, $\tilde{X}_{\theta} = D_{0.99}X_{\theta}$, $\tilde{Y}_{\theta} = D_{0.99}Y_{\theta}$, $\tilde{Z}_{\theta} = D_{0.99}Z_{\theta}$, where $D_{\alpha} = \text{diag}(1, \alpha, \alpha, 1)$. Clearly, even after accounting for the discrepancy between the average number of pulses per gate of these two RB protocols (n_N & n_C), the measured error rates still differ due to their differing sampling over the gate sets.

ing fixed (see figs. 3a and 3b) because they are sampling differently from the pulse sets, which causes them to probe different coherent error models. As such, it is bad practice to measure the scaled infidelity which is not equivalent to, and should not be confused with, the error per pulse.

IV. CONCLUSION

Randomized benchmarking (RB) is an important tool for estimating error rates associated with sets of elementary gate operations. SRB and NIST RB are two distinct RB protocols that have been confused in the literature and can lead to distinct outcomes. In this work we developed a rigorous theoretical framework proving that NIST RB, like SRB, leads to an exponential decay which depends only on the underlying gate-independent error model. We showed SRB, which samples from a uniform 2-design, and NIST RB, which samples from a subset of it, lead to significantly different observed error rates for a variety of physically realistic gate-dependent error models and pulse sets (see fig. 2). In typical cases the error rates differ by up to a factor of 3, which could have a significant impact on the overhead when implementing

fault-tolerant quantum error correction.

A next step is to develop a rigorous theoretical framework under which the experimental results from NIST RB and other RB methods using arbitrary gate sets can be analyzed in a unified and related to infer properties of the underlying error model in a consistent manner.

Acknowledgements

We thank Daniel Gottesman for fruitful discussions on QECC. This research was supported by the U.S. Army Research Office through grant W911NF-14-1-0103. This research was undertaken thanks in part to funding from TQT, CIFAR, the Government of Ontario, and the Government of Canada through CFREF, NSERC and Industry Canada.

Appendix A: NIST RB analysis under gate-dependent noise

In this section, we broadly justify the validity of NIST RB in the case of gate-dependent error models. Since a complete analysis would necessitate pages of mathe-

mathematical developments, we first suggest the reader to get familiar with [6, 8, 27, 32].

The essence behind the proof of the decay model eq. (3) resides in realizing that the RB recovery probabilities evolve as a combination of decays $\sum_i p_i^m$, where p_i are the eigenvalues of $\mathbb{E}_{\mathbf{N}}G \otimes \tilde{G}$. Those eigenvalues are slightly perturbed from those of $\mathbb{E}_{\mathbf{N}}G \otimes G$. In the case of the NIST gate-set \mathbf{N} , the non-zero eigenvalues are 1, 1, 1/2 and -1/2. In the perturbed case ($\mathbb{E}_{\mathbf{N}}G \otimes \tilde{G}$), the first eigenvalues remains 1, as it translates in the trace-preservation property, and the second one becomes $p_{\mathbf{N}} \approx 1$. The two eigenvalues which are close to $\pm 1/2$ decay very fast as the circuit grows, and don't contribute to the decay model for m large enough.

The relationship between the decay constant $p_{\mathbf{N}}$ and the infidelity $r_{\mathbf{N}}$ (eq. (4)) can be derived as a straightforward generalization of the analysis derived in [8]. Let the eigenvector related with the decay $p_{\mathbf{N}}$ be

$$\mathbb{E}_{\mathbf{N}}G \otimes \tilde{G} \text{vec}(L) = p_{\mathbf{N}} \text{vec}(L), \quad (\text{A1})$$

where $\text{vec}(\cdot)$ is the column vectorization. In a nutshell, eq. (4) holds as long as the singular values of L are close to each other, which is shown to be the case in 1-qubit SRB [8]. The reasoning, which pertains for the NIST gate-set, goes as follow. Let Π_{tr} be the 3×3 projector on the traceless hyperplane (the Bloch space). Given the spectrum of $\mathbb{E}_{\mathbf{N}}G \otimes \tilde{G}$, we have that:

$$L \approx \mathbb{E} \left(\frac{\tilde{G}_m \tilde{G}_{m-1} \cdots \tilde{G}_1 G_{m:1}^{-1}}{p_{\mathbf{N}}^m} \right) \Pi_{\text{tr}}, \quad (\text{A2})$$

for m large enough so the r.h.s converges. Indeed, performing $p_{\mathbf{N}}^{-1} \mathbb{E}_{\mathbf{N}} \Pi_{\text{tr}} G \otimes \tilde{G}$ multiple times converges very quickly to a rank-1 projector onto the desired eigenspace. Since L is the result of a reasonably short sequence of noisy operations (say $m = -2 \log(r) / \log(2)$), it is proportional to a high-fidelity channel, for which the singular values are close to each other (at least in the single-qubit case).

-
- [1] J. Emerson, R. Alicki, and K. Życzkowski, *Journal of Optics B: Quantum and Semiclassical Optics* **7**, S347 (2005).
 - [2] C. Dankert, R. Cleve, J. Emerson, and E. Livine, arXiv preprint quant-ph/0606161 (2006).
 - [3] B. Levi, C. C. Lopez, J. Emerson, and D. G. Cory, *Physical Review A* **75**, 022314 (2007).
 - [4] E. Magesan, J. M. Gambetta, and J. Emerson, *Physical Review Letters* **106**, 180504 (2011).
 - [5] E. Magesan, J. M. Gambetta, and J. Emerson, *Physical Review A* **85**, 042311 (2012).
 - [6] J. J. Wallman, *Quantum* **2**, 47 (2018).
 - [7] T. Proctor, K. Rudinger, K. Young, M. Sarovar, and R. Blume-Kohout, *Physical Review Letters* **119**, 130502 (2017), arXiv:1702.01853 [quant-ph].
 - [8] A. Carignan-Dugas, K. Boone, J. J. Wallman, and J. Emerson, *New Journal of Physics* (2018).
 - [9] R. Barends, J. Kelly, A. Veitia, A. Megrant, A. Fowler, B. Campbell, Y. Chen, Z. Chen, B. Chiaro, A. Dunsworth, *et al.*, *Physical Review A* **90**, 030303 (2014).
 - [10] A. Dugas, J. J. Wallman, and J. Emerson, *Physical Review A* **92**, 060302 (2015), arXiv:1508.06312 [quant-ph].
 - [11] A. W. Cross, E. Magesan, L. S. Bishop, J. A. Smolin, and J. M. Gambetta, *npj Quantum Information* **2**, 16012 (2016), arXiv:1510.02720 [quant-ph].
 - [12] J. J. Wallman, M. Barnhill, and J. Emerson, *New Journal of Physics* **18**, 043021 (2016).
 - [13] J. J. Wallman, M. Barnhill, and J. Emerson, *Physical Review Letters* **115**, 060501 (2015).
 - [14] E. Knill, D. Leibfried, R. Reichle, J. Britton, R. Blakestad, J. D. Jost, C. Langer, R. Ozeri, S. Seidelin, and D. J. Wineland, *Physical Review A* **77**, 012307 (2008).
 - [15] T. Xia, M. Lichtman, K. Maller, A. Carr, M. Piotrowicz, L. Isenhower, and M. Saffman, *Physical review letters* **114**, 100503 (2015).
 - [16] J. T. Muhonen, A. Laucht, S. Simmons, J. P. Dehollain, R. Kalra, F. E. Hudson, S. Freer, K. M. Itoh, D. N. Jamieson, J. C. McCallum, A. S. Dzurak, and A. Morello, *Journal of Physics: Condensed Matter* **27**, 154205 (2015).
 - [17] J. Kelly, R. Barends, B. Campbell, Y. Chen, Z. Chen, B. Chiaro, A. Dunsworth, A. G. Fowler, I.-C. Hoi, E. Jeffrey, A. Megrant, J. Mutus, C. Neill, P. J. J. O'Malley, C. Quintana, P. Roushan, D. Sank, A. Vainsencher, J. Wenner, T. C. White, A. N. Cleland, and J. M. Martinis, *Physical Review Letters* **112**, 240504 (2014).
 - [18] R. Barends, J. Kelly, A. Megrant, A. Veitia, D. Sank, E. Jeffrey, T. C. White, J. Mutus, A. G. Fowler, B. Campbell, Y. Chen, Z. Chen, B. Chiaro, A. Dunsworth, C. Neill, P. O'Malley, P. Roushan, A. Vainsencher, J. Wenner, A. N. Korotkov, A. N. Cleland, and J. M. Martinis, *Nature* **508**, 500 (2014), letter.
 - [19] D. C. McKay, S. Sheldon, J. A. Smolin, J. M. Chow, and J. M. Gambetta, arXiv preprint arXiv:1712.06550 (2017).
 - [20] S. Sheldon, L. S. Bishop, E. Magesan, S. Filipp, J. M. Chow, and J. M. Gambetta, *Physical Review A* **93**, 012301 (2016).
 - [21] J. E. Tarlton, *Probing qubit memory errors at the 10- 5 level*, Ph.D. thesis.
 - [22] K. R. Brown, A. C. Wilson, Y. Colombe, C. Ospelkaus, A. M. Meier, E. Knill, D. Leibfried, and D. J. Wineland, *Physical Review A* **84**, 030303 (2011).
 - [23] T. Harty, D. Allcock, C. J. Ballance, L. Guidoni, H. Janacek, N. Linke, D. Stacey, and D. Lucas, *Physical review letters* **113**, 220501 (2014).
 - [24] C. J. Wood and J. M. Gambetta, *Physical Review A* **97**, 032306 (2018).
 - [25] T. Chasseur and F. K. Wilhelm, *Physical Review A - Atomic, Molecular, and Optical Physics* **92**, 042333 (2015), arXiv:1505.00580v2.
 - [26] J. M. Gambetta, A. D. Córcoles, S. T. Merkel, B. R. Johnson, J. A. Smolin, J. M. Chow, C. A. Ryan,

- C. Rigetti, S. Poletto, T. a. Ohki, M. B. Ketchen, and M. Steffen, *Physical Review Letters* **109**, 240504 (2012).
- [27] T. J. Proctor, A. Carignan-Dugas, K. Rudinger, E. Nielsen, R. Blume-Kohout, and K. Young, *arXiv preprint arXiv:1807.07975* (2018).
- [28] S. Kimmel, M. P. da Silva, C. a. Ryan, B. R. Johnson, and T. a. Ohki, *Physical Review X* **4**, 011050 (2014).
- [29] J. Emerson, M. Silva, O. Moussa, C. A. Ryan, M. Laforest, J. Baugh, D. G. Cory, and R. Laflamme, *Science* **317**, 1893 (2007).
- [30] J. J. Wallman and J. Emerson, *Physical Review A* **94**, 052325 (2016).
- [31] E. Knill, *Nature* **434**, 39 (2005).
- [32] S. T. Merkel, E. J. Pritchett, and B. H. Fong, *arXiv preprint arXiv:1804.05951* (2018).
- [33] A. M. Meier, *Randomized Benchmarking of Clifford Operators*, Ph.D. thesis, University of Colorado, Boulder, CO (2013).
- [34] A. C. Dugas, J. J. Wallman, and J. Emerson, *ArXiv e-prints* (2016), *arXiv:1610.05296* [quant-ph].